ELSEVIER

Journal of Alloys and Compounds 300–301 (2000) 360–369

Journal of ALLOYS AND COMPOUNDS

www.elsevier.com/locate/jallcom

Synthesis and spectroscopic characteristics of a new class of lanthanide compounds of formulae $Ln(HX)_3(NO_3)_3$ and $Ln(HX)_3Cl_3$

Janina Legendziewicz[a,*], Grażyna Oczko[a], Vladimir Amirkhanov[b], Rafał Wiglusz[a],
V.A. Ovchynnikov[b]

[a]Faculty of Chemistry, University of Wrocław, F. Joliot-Curie Str. 14, 50-383 Wroclaw, Poland
[b]Institute of Chemistry, Kiev State University, Vladimirskaya 64, 2520033 Kiev, Ukraine

Abstract

Two series of the lanthanide (Eu, Pr) compounds of the formulae $Ln(HX)_3Cl_3$ (1); $Ln(HX)_3(NO_3)_3$ (2) [where $HX=CCl_3CO–NH–PO(NEt_2)_2$] with C.N.=6 and 9 were obtained in the form of monocrystals. The spectroscopic properties of these compounds were investigated at 293, 77 and 4.2 K and the results related to their structures. Correlation was made with the spectroscopic data and structure of the Eu and Nd respective chelates. Essential differences were found in coordination mode of ligand molecules in those systems. Intensity analysis of electronic transitions, electron–phonon coupling, as well as splitting and energies of electronic levels were used as tests of metal bonding in the systems under investigation. The electronic f–f transitions of praseodymium (1, 2) compounds show drastic differences in oscillator strength values, pointing thus at substantial differences in symmetry of the metal centre. Judd–Ofelt parameters were calculated with low errors of estimation. The relatively strong vibronic lines appear at displacement frequencies, corresponding to both ligand and $Ln–L_n$ localised vibrational modes. © 2000 Elsevier Science S.A. All rights reserved.

Keywords: Synthesis; Spectroscopy; Emission; Excitation; Eu(III); Pr(III); Intensity calculations

1. Introduction

Phosphoro-azo derivatives of β-diketones have been applied as anticancer agents [1,2]. However, the knowledge about the role of functional groups as well as their metal complexes in this process is not sufficient yet.

Recently we investigated the europium and neodymium complexes with three types of β-diketone derivatives [3–5]. Their structure and spectroscopic properties at 293, 77 and 4.2 K were reported [3,5]. The normal coordinate analysis was done and used in explanation of the IR and Raman data. It was found that depending on pH during complexation two types of compounds were formed, chelating ML_4 type (I) with strong M–L bond and relatively high covalency determined on the basis of the nephelauxetic effect that described by Jorgensen [6], and $M(HX)_3L_3$ type (II) with the protonated form of ligand molecule [7,8]. The lanthanide chelates of the first group exhibit biological activities and in vitro tests show their strong anticancer properties [5]. Crystal structure of the second group of complexes explained the kind of β-diketone bonding mode and formation of complexes with C.N.=6 and 9 with chloride and nitrate as a counterions.

The aim of the present studies is to focus on spectroscopic properties of the compound including electron–phonon coupling. The main purpose of this report is to show how the structural differences are reflected in the general features of the Eu(III) and Pr(III) optical absorption, excitation and emission spectra. The title compounds are excellent examples to such a analysis.

2. Experimental

Two types, $Ln(HX)_3Cl_3$ (1) and $Ln(HX)_3(NO_3)_3$ (2), of europium and praseodymium complexes were prepared according to the procedure described in details in [7,8] and were grown up in the form of single crystals of good optical quality and 1×2×3 mm dimensions.

Samples were checked by the X-ray methods and

---

*Corresponding author. Tel.: +48-71-320-4300; fax: +48-71-328-2348.
E-mail address: jl@wchuwr.chem.uni.wroc.pl (J. Legendziewicz)

0925-8388/00/$ – see front matter © 2000 Elsevier Science S.A. All rights reserved.
PII: S0925-8388(99)00766-5

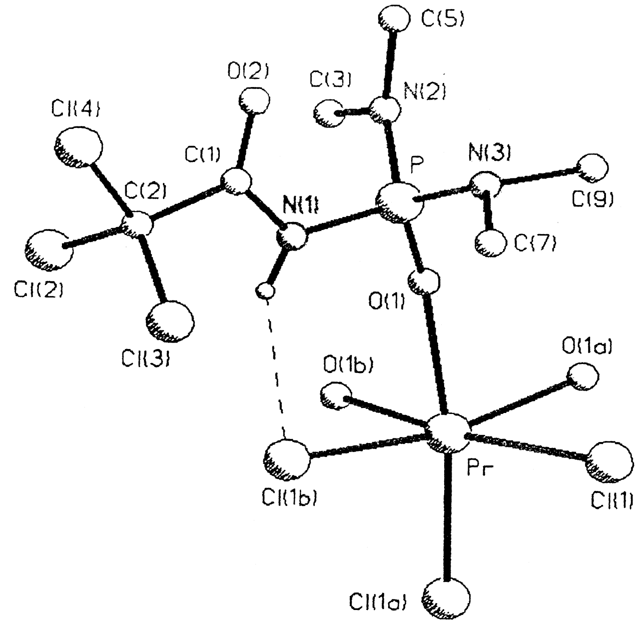

Fig. 1. Coordination polyhedron and type of the ligand coordination in the structure of $[PrCl_3\{CCl_3C(O)N(H)P(O)(NEt_2)_2\}_3]$ [7].

densities of crystals $\rho_1=1.495$ g cm^{-3}, $\rho_2=1.559$ g cm^{-3}, were used to determine of metal ions molar [M/l] concentrations.

The Drew method [9] was applied in the fitting procedure of coordination polyhedra for samples 1 and 2.

Absorption spectra were recorded on a Cary-Varian 5 spectrophotometer equipped with helium flow cryostat at 293, 50 and 4.2 K in 250–2200 nm spectral range. The intensities of optical lines in single crystal spectra were calculated on TAUS program, transformed to the oscillator strength values and applied to calculate the τ_λ Judd– Ofelt [10,11] parameters according to the procedure described in [12,13].

The excitation and emission spectra were recorded at 293 and 77 K using SLM Aminco SPF 500 spectrofluorimeter. Raman experiment was performed with spectrometer Nicolet 860 FTIR with Raman accessory.

3. Results and discussion

Figs. 1 and 2 show views of the structures of two types of Pr and Eu compounds with C.N. 6 and 9 [7,8]. In both types of compounds metal ions are coordinated to phosphoro-azo-derivatives of β-diketones by PO group of ligand molecules and chloride and nitrate ions complete the C.N. to 6 and 9. The nitrate group is bidendate and additionally forms hydrogen bonding with H atoms of N–H moiety of β-diketones stabilising the crystal structure.

Table 1 presents the results of the fitting procedure of coordination polyhedra of investigated single crystal (2) which will be important in our further consideration of spectral properties. The analysis of the bonds and angles of compound (1) points at formation of relatively high symmetry trigonal antiprism polyhedron for compound (1)

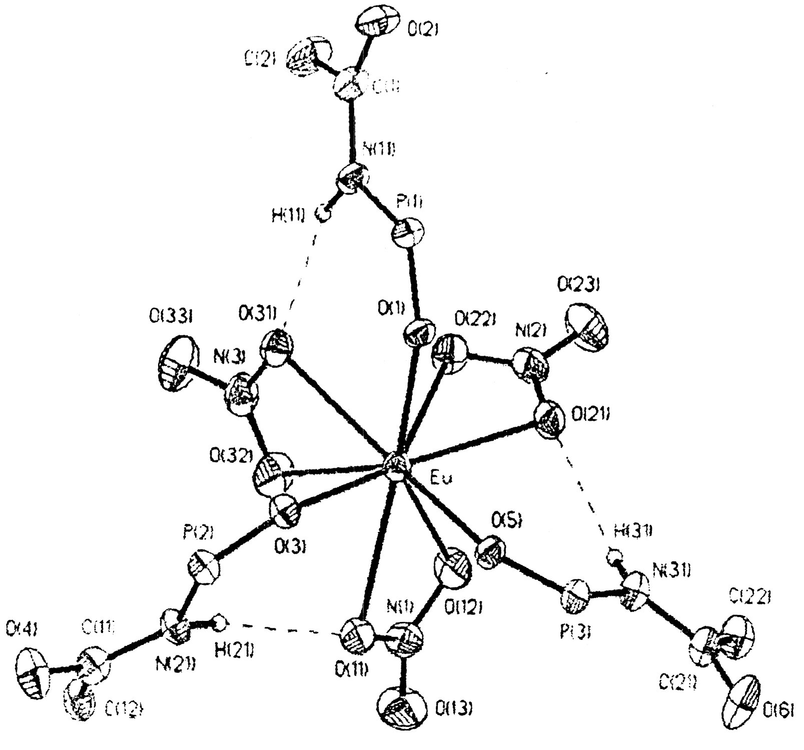

Fig. 2. Structure of $[Eu(NO_3)_3\{CCl_3C(O)N(H)P(O)(NEt_2)_2\}_3]$ (CCl_3 and NEt_2 groups are omitted) [8].

Table 1
Shape characteristics of polyhedra surrounding europium ion for compound (2)

	Δ tricapped trigonal prism	Δ capped square antiprism
Eu	0.19192	0.24301

whereas relatively low (C_{2V}) symmetry and C.N. 9 polyhedron in the case of the second compound.

Absorption spectra of praseodymium single crystals of (1) and (2) compounds at 293 and 4.2 K are presented in Figs. 3 and 4. The absorption bands observed correspond to transitions from praseodymium ground state multiplet $^3H_4$ to $^3H_6$, ^3F_J, $^1G_4$, $^1D_2$, ^3P_J and $^1I_6$ excited states. Note drastic differences in shapes and relative intensities of absorption bands in two types of compounds. Note also drastic differences in the number of Stark components in low temperature spectra of above single crystals. These differences will be manifested later in other spectroscopic properties of the systems investigated.

Let us consider first the room temperature spectra for 1 and 2 compounds. At room temperature, absorption spectrum of Pr (1) is complex and its intensity is mainly determined by strong electron–phonon coupling, allowed by relatively high symmetry. It is well manifested in the values of the oscillator strengths of f–f transitions collected in Table 2. Intensities of all transitions are almost two times lower (with the exception of IR region: $^3H_6$, $^3F_2$ levels) and drastic for $^3H_4 \rightarrow {}^3F_3$; $^3F_4$; $^3P_2$ transitions. In fact, $^3H_4 \rightarrow {}^3P_0$ bands exhibit the lowest intensities detected by us in the systems investigated up to now [14,15]. Intensity of $^3H_4 \rightarrow {}^3P_0$ transition in $Pr(HX)_3Cl_3$ spectra is comparable with that reported for high symmetry compounds by Richardson [16] and others [17,18].

The low temperature spectra confirm strong vibronic contribution in intensities of the both latter systems.

Decrease of temperature to 20 K leads to decrease of intensities, thus $^3H_4 \rightarrow {}^3P_0$ band disappears at 20 K of compound (1). In fact the strongest decrease of intensities was observed with decrease of temperature to 50 K in $^3H_4 \rightarrow {}^3F_2$ transition. Most probably it is the results of the largest dynamic to static ratios found for this transition by Richardson in trigonal symmetry [19]. Moreover, the number of components in low temperature spectra reduces meaningly in comparison to that observed in respective transitions of compound (2) mainly in the range $^3H_4 \rightarrow {}^3P_0$;

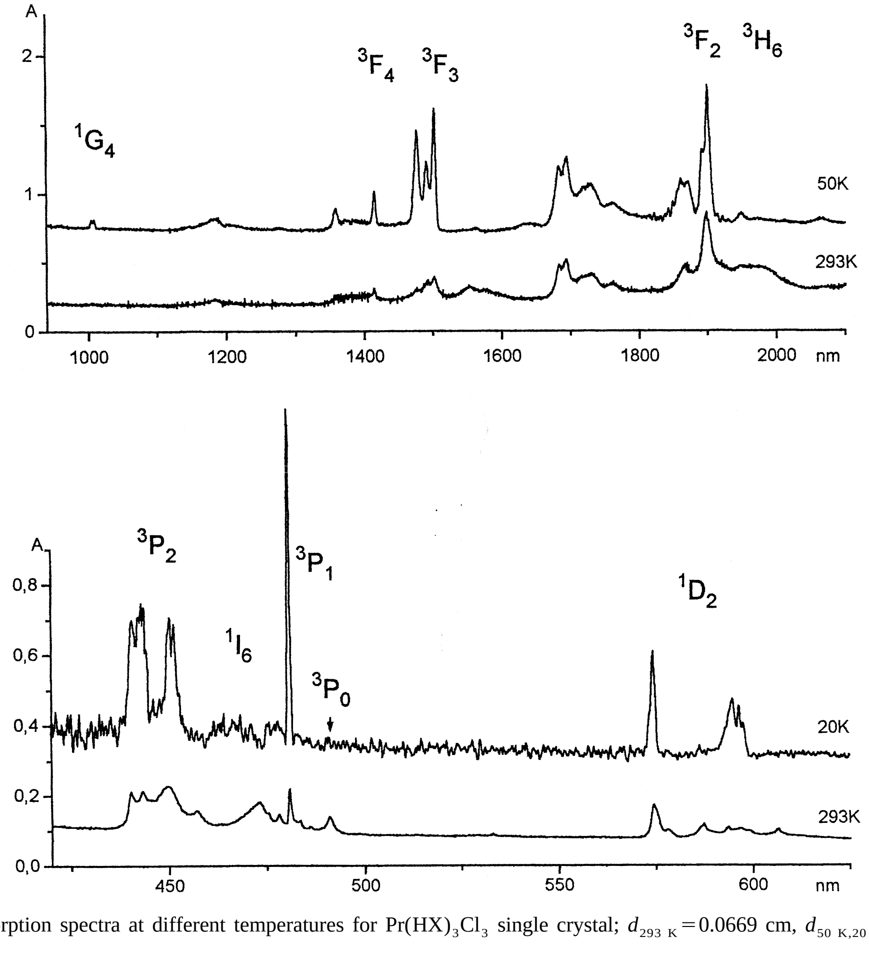

Fig. 3. Absorption spectra at different temperatures for $Pr(HX)_3Cl_3$ single crystal; $d_{293\ K} = 0.0669$ cm, $d_{50\ K, 20\ K} = 0.15$ cm.

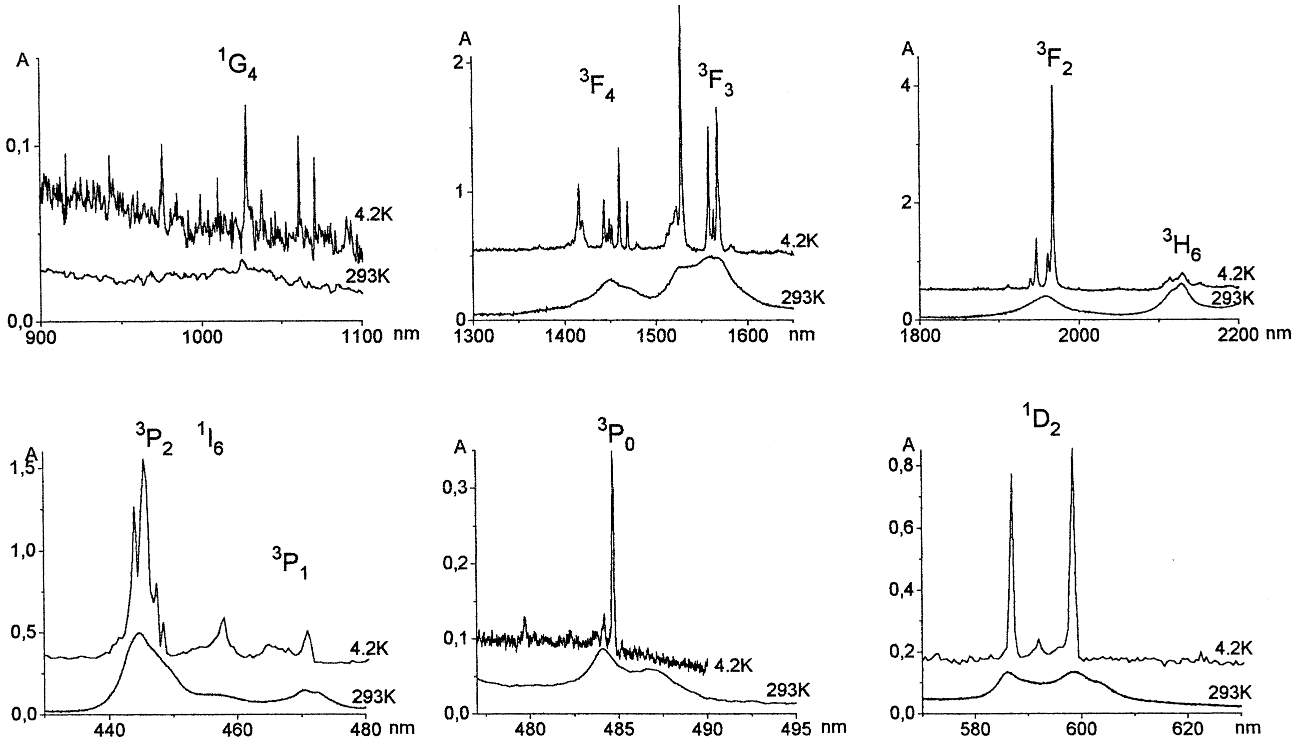

Fig. 4. Absorption spectra at different temperatures for $Pr(HX)_3(NO_3)_3$ single crystal; $d_{293\ K}=0.0659$ cm, $d_{4.2\ K}=0.0425$ cm.

$^3P_1$; $^3F_3$ and $^3F_4$ transitions. Other transitions need further analysis of the spectra recorded at 4.2 K for compound (1).

In the spectra of compound (2) at 4.2 K $^3H_4 \rightarrow {}^3P_0$ transition becomes single line and in other transitions Stark components correspond rather to C_{2V} symmetry of metal centre. Considering the results of the intensity calculation we found opposite to others relation of the intensity changes at low temperature for $^3H_4 \rightarrow {}^3P_2$ transition. Moreover, the strongest increase of intensities (the same order of oscillator strength values at 293 K) was observed for $^3H_4 \rightarrow {}^3F_3$ and $^3P_2$ transitions (although the first obeys magnetic dipole selection rule $\Delta J = 1$) in compound (2) compared to compound (1). Thus, $^3H_4 \rightarrow {}^3F_3$ transition exhibits hypersensitivity.

Table 2
Oscillator strength values of f–f transitions $P \cdot 10^{-8}$ and the $\tau_\lambda \cdot 10^{-9}$ parameter values for $Pr(HX)_3Cl_3$ and for $Pr(HX)_3(NO_3)_3$ single crystals

	$Pr(HX)_3Cl_3$ (1)		$Pr(HX)_3(NO_3)_3$ (2)	
$^3H_4 \rightarrow$	293 K	50 K	293 K	4.2 K
$^3H_6^3F_2$	739.73	204.55	709.06	645.06
$^3F_3$	325.56	215.42	1045.07	541.15
$^3F_4$	120.18	87.59	444.43	296.47
$^1G_4$	24.90	19.22	78.07	56.37
$^1D_2$	151.58	146.98	324.12	351.64
		154.39 20 K		
				64.96 15 K
$^3P_0$	47.38		89.07	42.92
$^3P_1$	251.17	175.92	302.33	256.54
$^1I_6$		159.78 20 K		
$^3P_2$	518.58	409.54	1448.85	1989.17
		384.92 20 K		
$\tau_2 \cdot 10^9$	20.89±5.02		9.14±11.16	
$\tau_4 \cdot 10^9$	4.38±2.34		6.75±5.04	
$\tau_6 \cdot 10^9$	4.33±2.01		19.88±4.49	

Oscillator strengths (collected in Table 2) evaluated from spectra at 293 K were further used to calculate the Judd τ_λ parameters. Unexpectedly Judd–Ofelt parameter calculation leads to quite good estimation of τ_λ parameters with relatively low errors especially for compound (1) (see Table 2).

Let us consider now the results of emission and excitation spectra at 293 and 77 K. Among the trivalent lanthanide ions, Eu^{3+} is especially useful as an optical probe of ligand or crystal field perturbations on 4f electron energy levels and radiative transition probabilities. The ground state multiplet $^7F_0$ and also principal emitting state $^5D_0$ is non-degenerated. Therefore $^7F_0 \leftrightarrow {}^5D_J$ absorption and emission spectra remain uncomplicated even at low symmetry. In some absorption spectra, however, the above transitions can be obscured by ligand to metal C–T transition.

Relative intensities of the $^7F_J \leftarrow {}^5D_0$ are of particular interest for characterising the mechanism responsible for 4f–4f radiative transition probabilities. Among these transitions, $^5D_0 \rightarrow {}^7F_1$ satisfies the intermediate-coupling magnetic dipole selection rule $\Delta J = 0, \pm 1$, only weakly dependent on C–F effects. On the other hand, to the first order in the odd-parity components of the C-F potential, only $^5D_0 \rightarrow ^7F_{2,4,6}$ are predicted to be electric dipole allowed in the absence of J-level mixings [20] and strong C-F dependent. The $^5D_0 \rightarrow ^7F_{0,1,3,5}$ can not acquire electric-dipole intensity until at least second order-first order in the odd-parity C-F components or by J-level mixing [21]. Thus, $^5D_0 \rightarrow ^7F_3$ emission exhibits mixed electric and magnetic dipole character, and their intensities (very weak) are also modulated by details of ligand environment. The $^5D_0 \rightarrow ^7F_{5,6}$ emission are generally very weak and almost undetectable.

Analysis of the Stark components in emission spectra and correlation with the number of electronic components of respective transition in excitation spectra with the same ΔJ allows to determine the D_3 symmetry for Eu (1) compound. Although in the X-ray report [7] ones of us suggested coordination polyhedra of Eu^{3+} ion close to distorted octahedra, our careful analysis of M–L distances and angles leads rather to trigonal antiprism polyhedron, and symmetry of metal centre close to D_3 (see Table 3) (it could be also treated as trigonal distortion of O_h symmetry). Thus, our analysis of spectral data well confirms above distortion. Similar procedure was applied to the

Table 3
Vibronic components in the emission spectrum of $Eu(HX)_3Cl_3$ ($^5D_0 \rightarrow ^7F_0$ and $^5D_0 \rightarrow ^7F_2$ transitions)

Transition	Energy (cm^{-1})		ΔE (from 0-phonon line)		
			1	2	3
$^5D_0 \rightarrow ^7F_0$	*17226*	(1)			
	17079		$147_{\delta OLnO}$		
	17074		$152_{\delta ClLnCl}$		
	17003		$223_{\nu Ln-Cl}$		
	16943		$283_{\nu LnO-(HX)}$		
	16775		$450_{\delta OPN}$		
	16758		$468_{\delta OPN}$		
$^5D_0 \rightarrow ^7F_1$	*16883*				
	16866				
$^5D_0 \rightarrow ^7F_2$	*16350*	(2)			
	16329		897		
	16252		974		
	16226				
	16218			$132_{\delta ClLnCl}$	
	16189			$161_{\delta OlnO}$	
	16149		1077		
	16131	(3)			
	16085		$1141_{\nu P=O}$		
	16051		1175	$299_{\nu LnO-(HX)}$	
	16033		1193	317	
	16003		1223	$347_{\nu LnOP}$	
	15972				$159_{\delta OLnO}$
	15901				$230_{\nu Ln-Cl}$
	15798		1428		$333_{\nu LnOP}$
$^5D_0 \rightarrow ^7F_3$	*15320*				
	15262				
	15204			$1146_{\nu P=O}$	
	15119				
	14991				$1140_{\nu P=O}$
$^5D_0 \rightarrow ^7F_4$	*14281*				
	14251				
	14213				
	14190				

Splitting of ^7F_J levels and activity of $^5D_0 \rightarrow ^7F_J$ transitions of Eu(III) in ligand fields

Symmetry	$J = 0$			$J = 1$			$J = 2$			$J = 3$			$J = 4$		
	Γ	ED	MD	Γ	ED	MD	Γ	ED	MD	Γ	ED	MD	Γ	ED	MD
D_3	A_1	–	–	A_2	+	+	A_1	–	–	A_1	–	–	$2A_1$	–	–
Number of				E	+	+	2E	+	+	$2A_2$	+	+	A_2	+	+
predicted lines										2E	+	+	3E	+	+
observed lines		1			2			2			4			4	

spectra of Eu (2), it shows C_{2V} symmetry of metal site (see Table 4) with strong distortion of TCTP polyhedra as it is seen from the results of the fitting procedure collected in Table 1.

Figs. 5 and 6 present emission and excitation spectra for two investigated systems. Next Fig. 7 shows the Raman spectra. Comparison of the emission spectra of two types of compounds with C.N. 6 and 9 in the range of 0–0 transition shows the low, almost undetectable band for crystal (1). It points at the D_3 group symmetry. In the range of 0–1 band two components with very low splitting (17 cm^{-1}) were found in the spectra of (1) and three very well resolved components in the low temperature spectra of (2) (splitting≈72 cm^{-1}). Their intensities are lower

Table 4
Vibronic components in the emission spectrum of $Eu(HX)_3(NO_3)_3$ ($^5D_0 \rightarrow {}^7F_0$ and $^5D_0 \rightarrow {}^7F_2$ transitions)

Transition	Energy (cm^{-1})		ΔE (from 0-phonon line)		
			1	2	3
$^5D_0 \rightarrow {}^7F_0$	*17232*	(1)			
	17100		$132_{\delta OLnO}$		
	17056		$176_{\delta OLnO}$		
	17036		$196_{\delta OLnO}$		
	17007		$226_{\nu LnO-(NO_3)}$		
	16949		$283_{\nu LnO-(HX)}$		
$^5D_0 \rightarrow {}^7F_1$	*16899*				
	16856				
	16827				
$^5D_0 \rightarrow {}^7F_2$	*16266*	(2)			
	16181				
	16142	(3)			
	16071		$1161_{\nu P=O}$		
	16051			$215_{\nu LnO-(NO_3)}$	
	15982			$283_{\nu LnO-(HX)}$	
	15943		$1289_{\nu_1(NO_3)}$		$199_{\delta OLnO}$
	15926			$215_{\nu LnO-(NO_3)}$	
	15634				$508_{\delta OPN}$
	15625				$517_{\delta OPN}$
	15576				$566_{\rho PNC}$
	15564			$702_{\nu_5(NO_3)}$	$578_{\rho PNC}$
	15541				$725_{\nu_3(NO_3)}$
	15444			$822_{\nu_6(NO_3)}$	$698_{\nu_5(NO_3)}$
$^5D_0 \rightarrow {}^7F_3$	*15376*				
	15308				
	15194				$1072_{\nu_2(NO_3)}$
	15128				
	15102				$1040_{\nu_2(NO_3)}$
	15055			$1138_{\nu P=O}$	
	14995				$1147_{\nu P=O}$
	14899				
	14863				
$^5D_0 \rightarrow {}^7F_4$	*14631*				
	14581				
	14531				
	14514				
	14409				
	14386				
	14219				

Splitting of ^7F_J levels and activity of $^5D_0 \rightarrow {}^7F_J$ transitions of Eu(III) in ligand fields

Symmetry	$J=0$			$J=1$			$J=2$			$J=3$			$J=4$		
	Γ	ED	MD	Γ	ED	MD	Γ	ED	MD	Γ	ED	MD	Γ	ED	MD
C_{2v}	A_1	+	−	A_2	−	+	$2A_1$	+	−	A_1	+	−	$3A_1$	+	−
				B_1	+	+	A_2	−	+	$2A_2$	−	+	$2A_2$	−	+
				B_2	+	+	B_1	+	+	$2B_1$	+	+	$2B_1$	+	+
							B_2	+	+	$2B_2$	+	+	$2B_2$	+	+

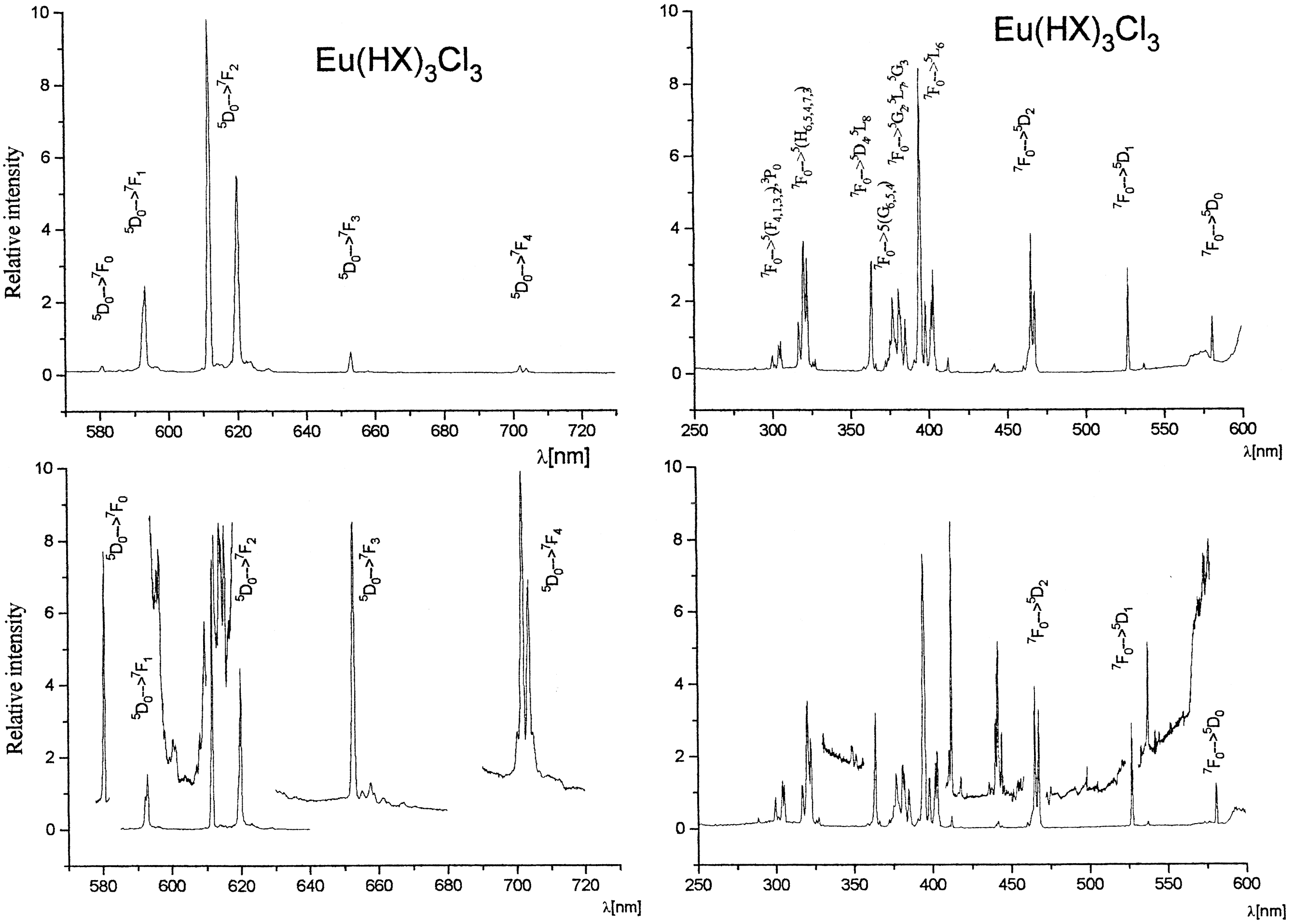

Fig. 5. Emission (left side) and excitation (right side) spectra for $Eu(HX)_3Cl_3$ at 77 K.

than $^5D_0 \rightarrow {}^7F_2$ ones in both the single crystals. In compound (1) two components separated by 219 cm^{-1} are observed, as well as relatively strong $^5D_0 \rightarrow {}^7F_3$ components. The $^5D_0 \rightarrow {}^7F_4$ transition, with even lower intensities than 0–3 band was also recorded. In spectra of (2), 4 strong and 1 weak components appear and reverse relation of intensities of 0–3 and 0–4 bands was observed.

The relatively strong 0–3 band in (1) can be attributed to significant crystal field induced J-level mixings between $^7F_2$ and $^7F_3$ levels.

The absolute intensities analysis will be possible after growing thicker crystals of sufficient optical quality.

Complex structure of bands in the range of 0–2 transition and additional small splitting of $^5D_0 \rightarrow {}^7F_1$ (6 cm^{-1}) Stark components could be caused by resonant effect involving vibronic components.

Electronic transitions at low temperature spectra are accompanied by vibronic components, which are mainly promoted by M–L localised modes: νM–O(NO_3), νM–Cl and M–O(HX) as well as internal ligand modes. Preliminary analysis of the vibronic components in emission and excitation spectra was performed in the range of $^7F_0 \leftrightarrow {}^5D_0$, $^5D_0 \rightarrow {}^7F_2$ and $^7F_0 \rightarrow {}^5D_2$ transitions and the results of assignments are collected in Tables 3–6. Comparing the vibronic transition probabilities in the title compounds spectra with those reported earlier for chelates with the same, but deprotonated ligands, the strongest vibronic components were promoted both by P=O and C=O modes and also π chelate modes coupled with νM–O ones. In the last considered compounds chelation leads to relatively strong covalency, nephelauxetic effect related to ionic doped Ln:(LaF_3) spectra is equal to 200 cm^{-1} whereas in the title compounds equals to 562 cm^{-1} and 296 cm^{-1} for praseodymium (III) $^3P_0$ level in compound (1) and (2), respectively. Full analysis of IR and Raman spectra as well as normal coordinate analysis will be the subject of next report.

4. Summary

1. High resolution absorption, excitation and emission spectra of two types of Pr and Eu compounds, $Ln(HX)_3Cl_3$ (1) and $Ln(HX)_3(NO_3)_3$ (2), were investigated at 293, 50 and 4.2 K.

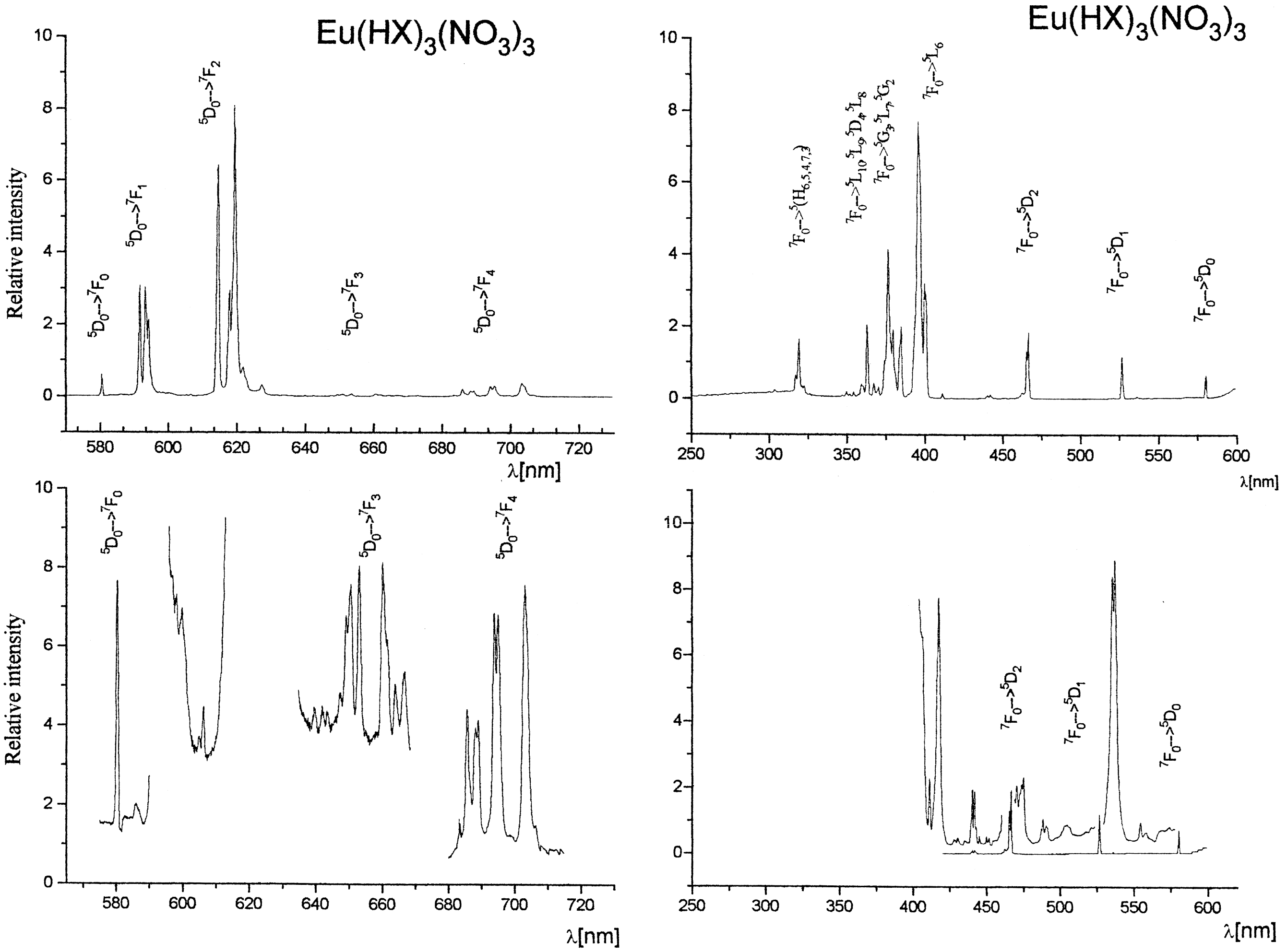

Fig. 6. Emission (left side) and excitation (right side) spectra for $Eu(HX)_3(NO_3)_3$ at 77 K.

Table 5
Vibronic components in the excitation spectrum of $Eu(HX)_3Cl_3$ ($^7F_0 \rightarrow {}^5D_0$ and $^7F_0 \rightarrow {}^5D_2$ transitions)

Transition	Energy (cm^{-1})		ΔE (from 0-phonon line) 1	2	3
$^7F_0 \rightarrow {}^5D_0$	*17226*	(1)			
	17346		$120_{\delta OLnO}$		
	17452		$226_{\nu Ln-Cl}$		
	17512		$283_{\nu Ln-O(HX)}$		
$^7F_0 \rightarrow {}^5D_2$	*21390*	(2)			
	21505	(3)			
	21575			$185_{\delta OLnO}$	
	21621			$231_{\nu Ln-Cl}$	
	21739			$349_{\nu LnOP}$	$234_{\nu Ln-Cl}$
	22547			$1157_{\nu P=O}$	$1145_{\nu P=O}$

Table 6
Vibronic components in the excitation spectrum of $Eu(HX)_3(NO_3)_3$ ($^7F_0 \rightarrow {}^5D_0$ and $^7F_0 \rightarrow {}^5D_2$ transitions)

Transition	Energy (cm^{-1})		ΔE (from 0-phonon line) 1	2	3
$2{}^7F_0 \rightarrow {}^5D_0$	*17226*	(1)			
	17430		$204_{Ln-O(NO_3)}$		
	17930		$704_{\nu_5(NO_3)}$		
	18237		$811_{\nu_6(NO_3)}$		
$^7F_0 \rightarrow {}^5D_2$	*21436*	(2)			
	21482	(3)			
	21621			$185_{\delta OLnO}$	$139_{\delta OlnO}$
	21715			$279_{\nu Ln-O(HX)}$	$233_{\nu Ln-O(NO_3)}$
	21953			$517_{\delta OPN}$	$471_{\delta OPN}$
	22142			$706_{\nu_5(NO_3)}$	
	22178			$742_{\nu_3\ (NO_3)}$	
	22224				$742_{\nu_3\ (NO_3)}$
	22471			$1035_{\nu_2(NO_3)}$	
	22573			$1137_{\nu P=O}$	
	22624				$1142_{\nu P=O}$
	22727			$1291_{\nu_1(NO_3)}$	
	22962			$1526_{\nu_4(NO_3)}$	$1480_{\nu_4(NO_3)}$

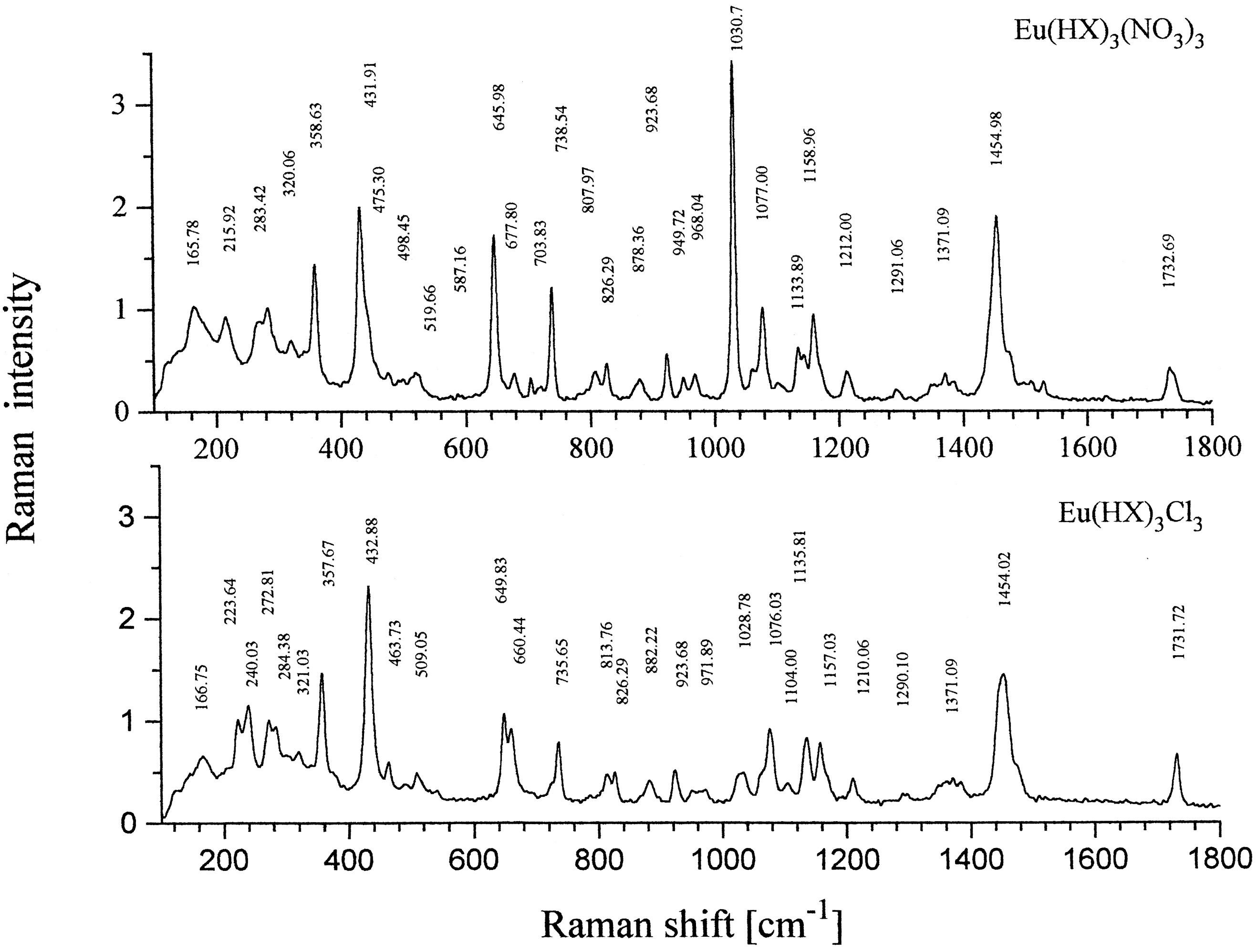

Fig. 7. Raman spectra for $Eu(HX)_3(NO_3)_3$ and $Eu(HX)_3Cl_3$.

2. Intensity analysis of f–f transitions for praseodymium compounds shows drastic differences in oscillator strength values for compounds (1, 2), pointing thus at drastic differences in symmetry of the metal centre. Judd–Ofelt parameters were calculated with relatively low errors of estimation.
3. The X-ray analysis revealed C.N. 6 and 9 for compounds 1 and 2, respectively. Fitting procedure of coordination polyhedra shows a deviation from the ideal TCTP polyhedron of Eu (2). Values of the oscillator strengths indicate the distortion of O_h symmetry of compound (1), what confirms well trigonal deviation toward the D_3 symmetry determined from the bonds and angles of X-ray results.
4. Strong decrease of intensity with temperature decrease in both the systems is due to relatively strong vibronic coupling and C–F effect.
5. Analysis of the number of Stark components in europium emission spectra allows us to assign the D_3 and C_{2V} point symmetry for metal centre in compound (1) and (2), respectively.
6. The P–O mode promotes the strongest vibronic components confirming thus coordination mode of ligand molecules, which corresponds well to the X-ray analysis.

References

[1] O.N. Riebrova, V.N. Biyushkin, T.I. Malinovshij et al., Dokl. A. N. UCCR 266 (1982) 1391.

[2] O.N. Riebrova, V.N. Biyushkin, L.D. Protsenko et al., Dokl. A. N. UCCR 274 (1984) 328.

[3] J. Sokolnicki, J. Legendziewicz, V. Amirkhanov, V. Ovchinnikov, L. Macalik, J. Hanuza, Spectrochim. Acta A 55 (1999) 349.

[4] V. Amirkhanov, C. Jañczak, L. Macalik, J. Hanuza, J. Legendziewicz, J. Appl. Spectrosc. 62 (1995) 5.

[5] V. Amirkhanov, V. Ovchinnikov, J. Legendziewicz, A. Graczyk, J. Hanuza, L. Macalik, Acta Phys. Polon. 90 (1996) 455.

[6] J.L. Ryan, C.K. Jorgensen, J. Phys. Chem. 70 (1966) 2845.

[7] V. Amirkhanov, V. Ovchinnikov, A. Kapshuk, V. Skopenko, J. Inorg. Chim. (Rus.) 40 (1995) 1869.

[8] V. Amirkhanov, A. Kapshuk, V. Ovchinnikov, V. Skopenko, J. Inorg. Chim. (Rus.) 41 (1996) 1470.

[9] M.G.B. Drew, Coord. Chem. Rev. 24 (1977) 179.
[10] R.B. Judd, Phys. Rev. 127 (1962) 750.
[11] G.S. Ofelt, J. Chem. Phys. 37 (1962) 511.
[12] J. Legendziewicz, K. Bukietyñska, G. Oczko, J. Inorg. Nucl. Chem. 43 (1981) 2393.
[13] J. Legendziewicz, Wiadomoœci Chem. 42 (1988) 605.
[14] G. Oczko, J. Legendziewicz, J. Hanuza, J. Gliñski, L. Macalik, Acta Phys. Polonica A 90 (1996) 431.
[15] J. Legendziewicz, G. Oczko, W. Strek, J. Hanuza, Eur. J. Solid State Inorg. Chem. 32 (1995) 95.
[16] F.S. Richardson, M.F. Reid, S.S. Dallara, R.D. Smith, J. Chem. Phys. 83 (1985) 3813, and references cited therein.
[17] W. Schartz, Mol. Phys. 31 (1976) 1909.
[18] A.K. Mukhopadhyay, M. Chowdhury, J. Chem. Phys. 67 (1977) 120.
[19] F.S. Richardson, J.D. Saxe, S.A. Davis, Th.R. Faulkner, Mol. Phys. 42 (1981) 1401.
[20] R.D. Peacock, Struct. Bonding 22 (1975) 83.
[21] A. Kirby, F.S. Richardson, Chem. Phys. Lett. 95 (1983) 507.